Laminar Stall Prediction and Estimation of $C_{L(\max)}$

Suresh H. Goradia* and Victor Lyman†
Lockheed-Georgia Co., Marietta, Ga.

A criterion for the prediction of laminar stall is developed from basic considerations of the laminar boundary layer theory. This criterion is applied to some NACA series 2-D airfoil sections and a 3-D wing that was wind tunnel tested. The correlation cases are presented for which freestream Mach number was approximately equal to 0.2 and freestream Reynolds number variations were in the range of 1 to 6 million. An estimation of $C_{L(MAX)}$ is made for cases where laminar stall is predicted. This criterion has been found useful both from the point of view of data analysis as well as for the design of a section of a 3-D wing for the purpose of delaying the occurrence of laminar stall. In addition, the criterion for the prediction of stall of a two-component airfoil with a leading edge slat is suggested.

Nomenclature

a = speed of sound
$C_1, C_2, C_3 - C_7$ = free constants appearing in Eq. (9)
C = airfoil chord
C_L = lift coefficient
C_P = pressure coefficient = $(P - P_\infty)/(\frac{1}{2}\rho U_\infty^2)$
K = $(\delta^2/\nu)(dU_e/dS)$
l = length of laminar bubble
M_e = local Mach number at the outer edge of boundary layer
n = correlation number = $-(\theta^2/\nu)(dU_e/dS)$
N = momentum parameter = $2[n(H + 2) + (\theta/U_e)(\partial u/\partial y)_w]$
P = static pressure
$R_{e\theta}$ = Reynolds number based on local momentum thickness = $(U_e\theta/\nu)$
Pr = Prandtl number
S = coordinate along the airfoil surface
u = longitudinal velocity component in boundary layer
U_e = velocity at the edge of the boundary layer
U_i = average velocity at slat exit
X = distance along the chord
Y = distance normal to the chord
δ = over-all boundary-layer thickness
δ^* = boundary layer displacement thickness = $\int_0^\delta [1 - (u/U_e)]dy$
η = dimensionless distance normal to airfoil surface = y/δ
θ = $\int_0^\delta (\rho u/\rho_e U_e)(1 - (u/U_e))dy$
θ_e = momentum thickness at slat exit on upper surface
θ_{iu} = momentum thickness at end of slat lower surface
θ_{iL} = momentum thickness on the upper surface of main component at slat end
μ = dynamic viscosity
ν = kinematic viscosity, u/ρ
ρ = density
τ_0 = wall shear stress

Subscripts

e = external edge of boundary layer
ore = slat exit
i = average at slat exit
o,w = conditions at wall
∞ = freestream conditions

Received July 9, 1973; revision received May 16, 1974. Considerable credit is due D. M. Ryle, B. H. Little, and T. Dansby of Lockheed-Georgia Company for their support and advice.

Index categories: Aircraft Aerodynamics (Including Component Aerodynamics); Boundary Layers and Convective Heat Transfer—Laminar; Boundary Layers and Convective Heat Transfer—Turbulent.

*Research, Design and Development Engineer.
†Scientist-Associate. Associate Member AIAA.

I. Introduction

STUDY of the evolution of wing lift as a function of incidence has shown in many instances the presence of bubble separation at the airfoil leading-edge resulting in laminar section stall. Experimental data on two-dimensional "peaky" airfoil sections indicate that $C_{L(MAX)}$, as limited by laminar stall, is strongly dependent on leading edge shape and freestream Reynold's number. The laminar boundary layer which develops on the upper surface of the airfoil at high angles of attack is subjected to a very high adverse pressure gradient after traveling only a short distance downstream. As a result, the local boundary-layer momentum thickness Reynold's number, $U_e\Theta/\nu$, just after the pressure peak, has not reached a level sufficiently high to cause transition to a turbulent boundary layer. On the other hand, the laminar boundary layer, because of its low kinetic energy level, has insufficient energy to surmount the "pressure hill" of the adverse pressure gradient near the leading edge. The result is that the laminar boundary layer separates from the surface of the airfoil. The separated shear-layer which is formed may curve back onto the airfoil surface within a short distance. This region of circulatory motion underneath a separated flow, between points of separation and reattachment, is defined as "short bubble." In certain cases, however, the separated viscous layer, which is formed in the neighborhood of the location of minimum peak pressure on the airfoil, may not reattach to the surface at all or may reattach after 0.2 to 0.3 chord lengths downstream. In either case, the flow over the airfoil is unsteady because of the presence of the large region of circulatory motion underneath the separated flow. The extended separated region is defined as "long separation bubble."

The presence of the short laminar separation bubble near the leading edge of the airfoil may give rise to laminar stall. This type of stall is distinguished from the turbulent or trailing edge stall by the fact that in the case of trailing edge stall, turbulent boundary-layer separation takes place near the aft end of the airfoil causing the existence of a sizeable region of separated flow. Figure 1 shows a typical pressure distribution for single-component airfoil exhibiting either laminar or trailing edge stall. Laminar stall is caused as a result of the presence of a very high pressure peak and succeeding high adverse pressure gradient near the leading edge where as trailing edge stall occurs as a result of a relatively high aft pressure gradient near the aft part of the airfoil. Figure 2 shows the typical lift curves for the airfoils exhibiting laminar short bubble stall, laminar long bubble stall, and turbulent or trailing edge stall for single component airfoils. The sharp break in the $C_L - \alpha$ curve for the airfoil exhibiting lami-

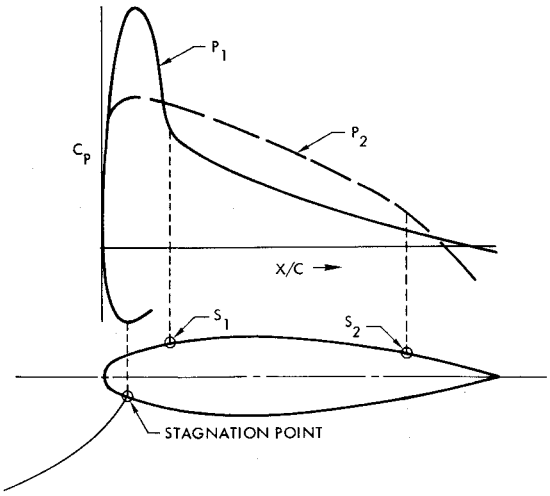

Fig. 1 Shape of the pressure distribution near stall where P_1 = pressure distribution for incipient laminar stall (short bubble and long bubble); P_2 = pressure distribution for incipient turbulent stall (trailing edge stall); S_1 = point of incipient laminar separation and reattachment or laminar separation only; and S_2 = point of incipient turbulent separation.

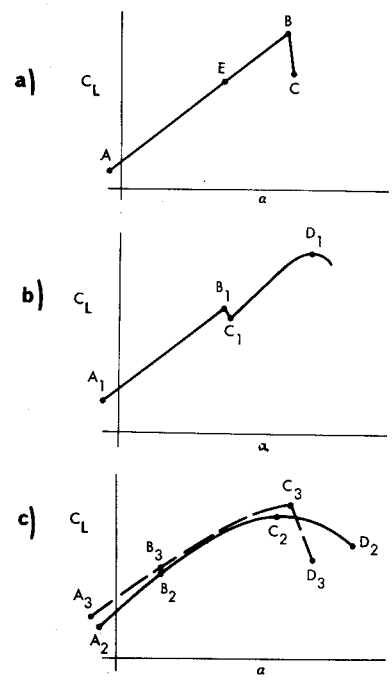

Fig. 2 Typical Airfoil staff patterns. a) Laminar short bubble short bubble at S_1 bursts and C_L drops abruptly from B to C; b) Laminar long bubble short bubble at S_1 develops into extended region of separation for C_L's between C_1 and D_1, flow is unstable; c) Turbulent trailing edge stall. $A_2B_2C_2D_2$ boundary layer changes from laminar to transition to turbulent and then separates at C_2. $A_3B_3C_3D_3$ boundary layer progresses from laminar to local separation then to turbulent reattachment and finally to turbulent separation.

nar short bubble stall is due to the sudden burst of the bubble near the leading edge of the airfoil at an angle of attack α_B; the separated shear layer near leading edge does not reattach to the airfoil surface at an angle of attack $\alpha > \alpha_B$. In the case of laminar long bubble stall, the airfoil has $C_L - \alpha$ characteristics as shown in Fig. 2b. In this case there is a break in the $C_L - \alpha$ curve at B_1; however, lift coefficient continues to increase with increase in $\alpha > \alpha_{B(1)}$. Because of the existance of the large region of separation, flow over airfoil is unsteady for angles of attack greater than $\alpha_{B(1)}$, and is therefore not representative of the steady flow conditions considered in this paper. The lift curve for the airfoil section exhibiting trailing edge stall is relatively smooth compared to sections exhibiting laminar stall; this is shown in Fig. 2c.

II. Related Investigations

Apart from the observation of Jones,[1,2] who was the first to recognize these bubble formations over 38 years ago, little work was carried out on the problem concerning separation bubbles until fresh interest was aroused through the use of thin airfoil sections for improving drag divergence Mach numbers at transonic speeds. von Doenhoff,[3] suggested certain reattachment criteria based on simple geometrical arguments. His subsequent method for predicting bubble bursting did not appear to be applicable to the general case. McGregor,[4] experimentally investigated leading-edge bubbles and hypothesized that the change in kinetic energy in going from the shear layer to the bubble must balance the losses due to viscous dissipation. Bubble expansion appeared to be a likely mechanism for maintaining this equilibrium. Owen and Klafner,[5] analyzing experimental pressures on several airfoils found that leading-edge bubbles could be typified as either "long" or "short" depending upon whether the separation boundary-layer Reynolds number ($R_{e(\delta^*)}$) was larger than or less than about 450. Crabtree,[6,7] correlating a large amount of experimental data by plotting log l/δ^* against $R_{e(\delta^*)}$, confirmed the existence of a critical Reynolds number of about 450–500 separating the two bubble regimes. Experimental cases have been found, however, which show much larger bursting Reynolds numbers (1200 for a blunt-nosed model) and some attempt has been made to explain these differences through consideration of the pressure rise over the bubble, for example in Ref. 6.

From the foregoing discussion, it is apparent that the presently available analytical techniques for predicting short or long bubble formation, as well as laminar stall, are useful for data correlation only; this is due in part to the many simplifying assumptions in the calculation of laminar boundary layer parameters. An attempt was made within the program framework of Ref. 14 to correlate a criterion for laminar stall prediction as suggested by Ref. 8 with erratic results. Consequently, the Goradia-Lyman criterion for the prediction of laminar stall on single-piece airfoils was developed for incorporation into computer program framework of Ref. 14. In this development, certain dimensionless parameters, comprising the laminar stall criterion, were derived by dimensional analysis. The actual relationship existing between the selected parameters was subsequently determined through correlation with experimental data. In the paragraphs which follow, the derivation of the laminar stall criterion through the dimensional analysis technique is outlined. In addition, suggested criterion for $C_{L(MAX)}$ of a two component airfoil with leading edge slat are derived from dimensional analysis. Correlation for $C_{L(MAX)}$ prediction for a case is illustrated for a two component airfoil with a leading edge slat.

III. Theoretical Study

In this section criteria for the prediction of $C_{L(MAX)}$ of a single component airfoil due to laminar stall and $C_{L(MAX)}$ for a two-component airfoil with a leading edge slat are presented. These criteria are derived with the use of dimensional analysis and by the application of principles of local dynamic similarity. However, the use of these criteria for the prediction of airfoil stall requires the knowledge of local boundary-layer momentum thickness development on the surface of the airfoil. For the application of criteria presented in this paper, it is necessary to calculate the

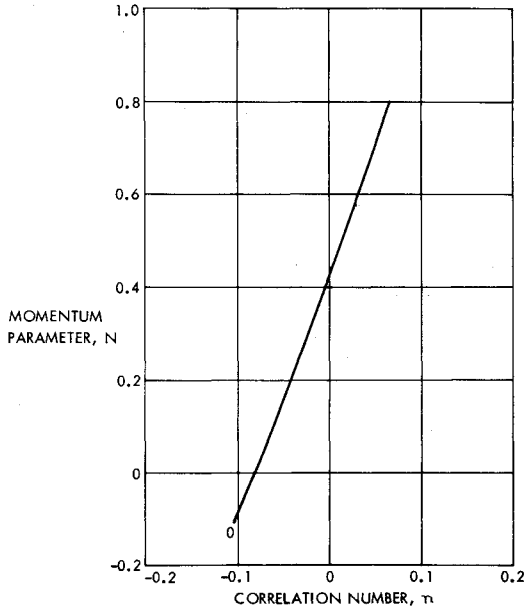

Fig. 3 Correlation number vs momentum parameter.

laminar-boundary layer momentum thickness distribution in the case of a single component airfoil, whereas for a two-component airfoil, both laminar and turbulent boundary-layer momentum thickness knowledge is required on the slat surfaces.

A. Summary of Equations for Calculating Laminar and Turbulent Boundary-Layer Development

The detailed derivation of these equations is given in Refs. 14 and 23. However, pertinent equations are as follows.

Laminar Boundary-Layer Equations

The reduced momentum integral equation for the laminar boundary layer is given by

$$-U_{e_{(x)}}\frac{d}{dx}\left(\frac{n}{\frac{dU_{e_{(x)}}}{dx}}\right) = N(x) \qquad (1)$$

where n = correlation number $= -(\Theta^2/\nu)(dUe/dx)$ and N = momentum parameter

$$= 2\left[n(H+2) + \frac{\theta}{U_e}\left(\frac{\partial u}{\partial y}\right)_\omega\right]$$

Relation between momentum parameter $N(n)$ and correlation number n, which is derived from the results of a similar solution of Cohen and Reshotko[13] is shown in Fig. 3. Integration of Eq. (1) for a given chordwise velocity or pressure distribution on the airfoil is done along the curve of Fig. 3 from the stagnation point to the point of theoretical laminar separation. The theoretical laminar separation point occurs when the value of separation correlation number reaches $n_{sep} = 0.069$.

The relation between laminar boundary-layer momentum thickness and the correlation number, which is valid at low subsonic Mach numbers is given as follows:

$$\theta_{(x)} = \left(\frac{c}{a_0}\nu_0\left(-n \div \frac{dM_e}{d(s/c)}\right)(1+2M_e^2)^4\right)^{1/2} \qquad (2)$$

The laminar boundary-layer form factor is calculated by the following empirical expression. This expression, which is valid at low subsonic Mach numbers, has been derived from the correlation of laminar boundary-layer data on several airfoils and is given by

$$H = [-1.1138n + 2.384(1 + 0.236M_e^2)] + 0.210(P_r)^{1/2}M_e^2 \qquad (3)$$

Turbulent Boundary-Layer Equations

The momentum thickness growth for the turbulent boundary layer on both upper and lower surfaces of the slat and downstream of the point of transition is calculated by the following equation:

$$\theta_{(x)} = \left[(\theta_i)^{1.17}\left(\frac{U_{ei}}{U_e}\right)^{3.51}\left(\frac{\nu}{\nu_i}\right)^{0.167} + \frac{0.00792\,\nu^{0.17}}{(U_e)^{3.51}}\int_{xi}^{x}(U_e)^{3.332}dx\right]^{1/1.17} \qquad (4)$$

where the subscript i refers to the conditions at the point of transition from a laminar to a turbulent boundary layer.

The turbulent boundary-layer form factor H is calculated by the simultaneous use of the following equations. These equations are derived by the use of momentum integral equations, a power law velocity profile assumption, and proper empirical modifications. Thus

$$\frac{d\tilde{H}}{dx} = \left[\frac{0.123}{\left(\frac{U_e\theta}{\nu}\right)^{0.17}} - \tilde{H}\left(\frac{\tau_W}{\rho U_e^2}\right) + (H-1.1)\frac{H}{U_e}\theta\frac{dU_e}{dx}\right]/\theta \qquad (5)$$

The form factor $\tilde{H}$, based on the dissipation energy thickness and appearing in the above equation is related to the usual form factor H by,

$$\tilde{H} = (1.269\,H/H - 0.379) \qquad (6)$$

and the wall shear appearing in Eq. (5) is calculated by the use of Ludwieg-Tillman shear stress expression. Figures 4 and 5 show the correlation of the results calculated by the use of the above equations with boundary-layer experimental data on airfoils. Figure 4 shows the plot of calculated values of momentum thickness Θ and form factor H in the laminar boundary-layer region and Fig. 5 shows the plot of the above parameters in the turbulent boundary layer region over an airfoil surface; experimental data on these airfoils are also shown plotted for comparison.

B. $C_{L(MAX)}$ Criterion for Single Component Airfoil

The point of theoretical laminar separation occurs when the value of correlation number n becomes approximately equal to 0.069. On the surface of an airfoil under usual conditions, the point of theoretical separation is preceded by the transition to a turbulent boundary layer. However, under those circumstances when the point of theoretical laminar separation is predicted instead of transition on the surface of the airfoil, it would be of interest to predict, in addition, the conditions under which the separated boundary-layer flow will reattach to the surface of the airfoil and conditions under which no reattachment is possible.

The physical parameters which may provide the indication as to whether or not the separated laminar shear layer may reattach to the surface of the airfoil in a short distance can be arrived at from the following theoretical analysis. The von Kármán momentum integral equation

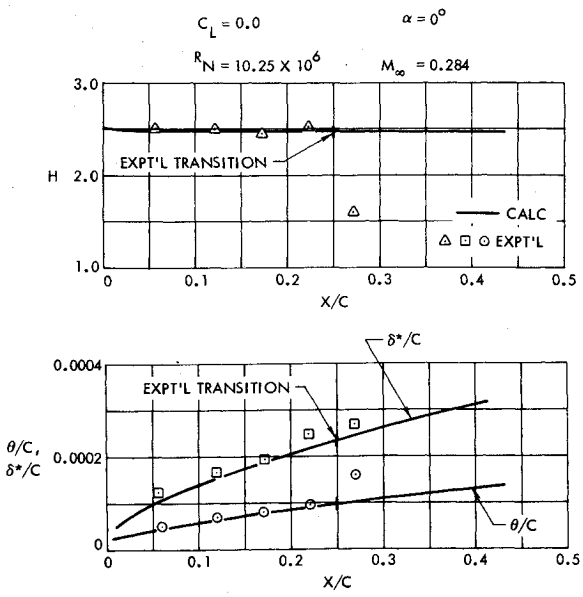

Fig. 4 Laminar boundary-layer correlation. NACA 0012.[24]

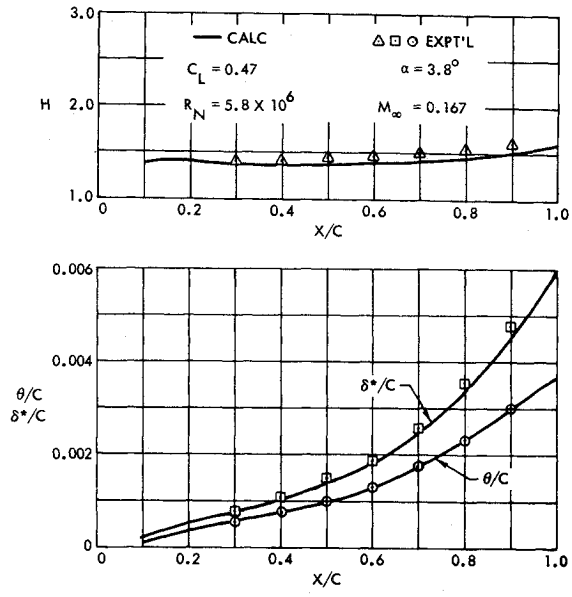

Fig. 5 Turbulent boundary-layer correlation. NACA 63-012.[16]

for a laminar boundary layer under the influence of an arbitrary pressure distribution is written as

$$\nu \frac{\partial u}{\partial y}\Big|_{y=0} = U_e^2 \frac{d\theta}{dS} + (2\theta + \delta^*) U_e \frac{dU_e}{dS} \tag{7}$$

Pohlhausen[9] introduced the following dimensionless quantities in his approximate laminar boundary-layer method

$$K = \frac{\delta^2}{\nu} \frac{dU_e}{dS} \quad n = \frac{\theta^2}{\nu} \frac{dU_e}{dS} \tag{8}$$

By choosing a fourth-order velocity profile for the laminar boundary-layer flow and the use of appropriate boundary conditions, the relations between various dimensionless laminar boundary-layer parameters, after Holstein and Bohlen,[10] can be expressed as

$$\begin{aligned} \frac{\delta^*}{\delta} &= C_1 + C_2 K \\ \frac{\theta}{\delta} &= C_3 + C_4 K + C_5 K^2 \\ n &= (C_3 + C_4 K + C_5 K^2)^2 K \\ H &= \frac{C_1 + C_2 K}{C_3 + C_4 K + C_5 K^2} = F_1(K) \text{ or } F_2(n) \end{aligned} \tag{9}$$

and

$$\frac{\tau_0 \theta}{\mu U_e} = (C_6 + C_7 K)(C_3 + C_4 K + C_5 K^2)^2 = F_{3(n)}$$

where C_i for $i = 1, 2 - 7$ are numerical constants.

For the purpose of establishing an empirical criterion for the presence of a laminar short or long bubble (i.e., for the prediction of laminar stall) various pairs of physical parameters which are shown in Eq. (9) may be selected. For example, the pair, H (or δ^*/Θ) and the pressure gradient parameter [or $(\delta^2/\nu)(dU_e/dS)$] could be chosen. The form factor, H, is used extensively in predicting separation for the turbulent boundary layer and also trailing edge stall on single component airfoils. This parameter, however, cannot be used in the case of laminar stall prediction because the measurement of velocity profiles downstream of the pressure peak in the adverse pressure gradient show an inconsistent variation of H as associated with transition phenomena. On the other hand by considering the combination $(\tau_0\Theta/\mu U_e)$ and n from Eq. (9), a source pair is obtained which, after the following simplification, provides the desired correlation parameters for the prediction of onset of laminar stall. Thus we have

$$\frac{\tau_0 \theta}{\mu U_e} \sim \frac{\theta^2}{\nu} \frac{dU_e}{dS}$$

where

$$\tau_0 = \mu \frac{\partial u}{\partial y}\Big|_{y=0}$$

or

$$\frac{\partial (u/U_e)}{\partial (y/c)} \cdot \frac{U_e}{c} \frac{\theta}{U_e} \sim \frac{\theta^2}{\nu} \frac{dU_e}{dS}$$

or

$$\frac{\partial (u/U_e)}{\partial (y/c)} \frac{\nu}{U_e \theta} \sim \frac{1}{U_e} \frac{dU_e}{d(s/c)} \tag{10}$$

Experimental measurements indicate that there is little change in the shape of velocity profiles, when plotted in the form of u/U_e vs y/c, in the vicinity of bubble formation on the upper surface of airfoils at high angles of attack. Furthermore, measurements also indicate that the phenomena of separation and possible reattachment of the laminar shear layer occurs just downstream of the location of pressure peak in its immediate vicinity. Hence, the dimensionless slope of velocity profile at the surface of the airfoil, i.e., $\partial(u/U_e)/\partial(y/c)$, can be regarded as approximately constant for the purpose of determining the separation reattachment criterion. Hence, the proportionality Eq. (10) can be written as

$$\frac{\nu}{U_e \theta} \sim \frac{1}{U_e} \frac{dU_e}{d(S/C)} \sim \frac{1}{M_e} \frac{dM_e}{d(S/C)} \tag{11}$$

where C is the chord of the airfoil. In the derivation of the above proportionality equation it is assumed that both free stream Mach number and local Mach numbers are sufficiently low, i.e., $M_e \lesssim 0.3$, that the effects of compressibility can be assumed as negligible.

Equation (11) derived by above dimensional analysis of laminar boundary-layer behavior, suggests that a pair of

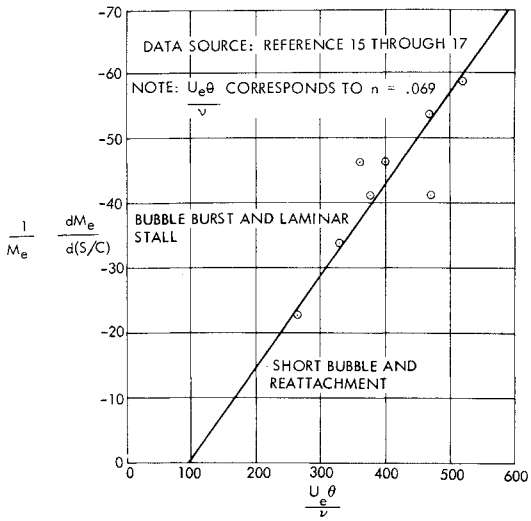

Fig. 6 Goradia-Lyman criterion for laminar stall prediction.

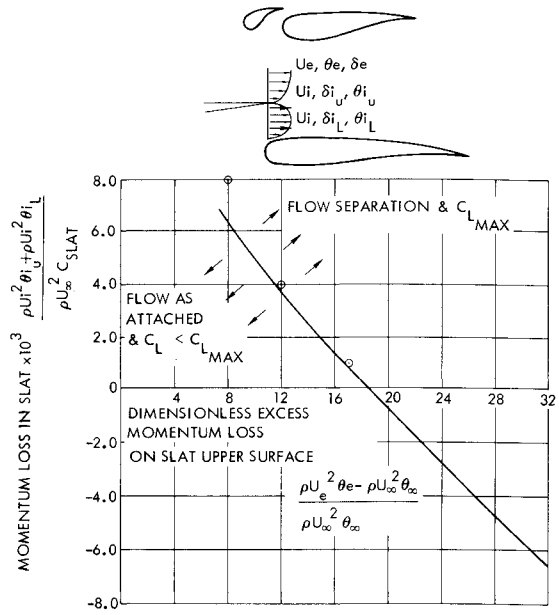

Fig. 8 Suggested criterion for $C_{L(MAX)}$ prediction for two-component airfoils with leading edge device.

parameters, such as the quantity $(1/M_e)/(dM_e/d(S/C))$ and local momentum thickness Reynolds number $R_e\Theta$, can be used for the purpose of predicting laminar stall. The result of the above analysis is different from that of Owen and Klafner[5] and Crabtree[6] in that these authors postulate from the analysis of their experimental data that the specification of a certain value Reynolds number based on either local momentum thickness or displacement thickness at the laminar separation point is sufficient for predicting the existence of reattachment phenomena. The present analysis, however, indicates that both pressure gradient and local momentum thickness Reynolds number at separation point determine the existence reattachment phenomena of the separated laminar shear layer. Figure 6 shows a curve for predicting laminar stall on a single-component airfoil. These curves have been obtained by the least-square straight line fit of the experimental velocity profile data in the vicinity of the bubble region along with the theoretical pressure gradient on the surface of the airfoil. This laminar stall criterion of Fig. 6 is used in conjunction with theoretical potential flow pressure distribution method which is described in Ref. 14 for the correlation of laminar stall prediction on airfoils described in this paper.

Figure 7 presents the logic used in determining the behavior of the laminar boundary layer when it reaches an instability condition. As the flow chart shows, the laminar boundary-layer calculation first checks for laminar instability with the Schlicting-Ulrich[11] instability curve of Fig. 7(a). If the laminar boundary layer is unstable, then Granville's criterion[12] is used for checking transition to a

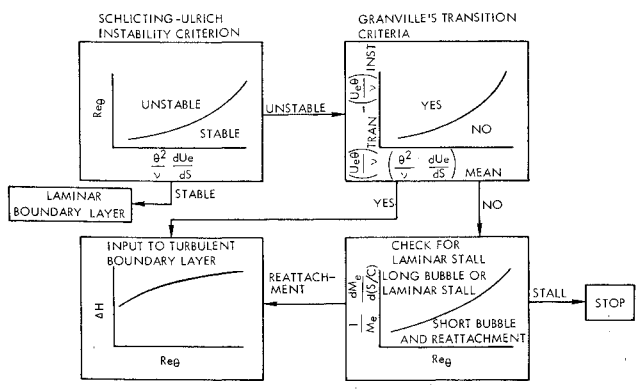

Fig. 7 Boundary-layer stability/separation calculation sequence.

turbulent boundary layer. Unless transition is indicated, in which case a turbulent boundary-layer calculation begins, a check is made for laminar separation, when $n = 0.069$ with the criterion of Fig. 3. Then, the criterion of Fig. 6 will tell whether a short or long separation bubble has occurred. The calculation proceeds to the turbulent boundary-layer routine with a short bubble but stops with the indication of a long bubble and stall.

C. $C_{L(MAX)}$ Criterion for a Two-Component Airfoil with a Leading Edge Device

Figure 6 shows the $C_{L(MAX)}$ criterion for predicting laminar stall for single-component airfoils. This semiempirical criterion, which was established from dimensional analysis and experimental velocity-profile data, has been successfully used for predicting $C_{L(MAX)}$ for single-piece airfoils and also in the design of clean wing sections for delaying laminar stall. However, this criterion when used for two-component airfoils with a leading edge device predicts stall at quite lower angles of attack. In the case of two-piece airfoils with a leading edge slat, the flow through the slot between the leading edge device and the aft component may, in addition, energize the boundary layer on the main component. Thus, the flow separation on the main component is suppressed and the angle of attack for stall is delayed for a system with leading edge devices.

Figure 8 shows the criterion for predicting $C_{L(MAX)}$ of a two-component airfoil section with a leading edge device. The theoretical basis and dimensional analysis for arriving at this criterion is briefly described as follows.

Momentum loss due to retarded flow in the boundary layer can be written as

$$\text{Momentum loss in B.L.} = U_e \int_0^\delta \rho u\,dy - \int_0^\delta \rho u^2\,dy$$

$$= \rho U_e^2 \int_0^\delta \frac{u}{U_e}\left(1 - \frac{u}{U_e}\right)dy$$

$$= \rho U_e^2\theta \qquad (12)$$

Boundary-layer separation and hence $C_{L(MAX)}$ is therefore dependent on the following momentum losses at the slow exit

$$C_{L_{(MAX)}} = F(\rho U_e^2\theta_e, \rho U_i^2\theta_{iu}, \rho U_i^2\theta_{iL})$$

where Θ_e = momentum thickness at the trailing edge of slat upper surface, Θ_{iu} = momentum thickness at the end of the slat lower surface, Θ_{il} = momentum thickness on the upper surface of main component at the slot exit, U_e = velocity at the trailing edge of the upper surface of the slat, and U_i = average velocity at the exit of the slat.

From the physical reasoning it can be shown that the load carried by the slat is in proportion to the following parameter, i.e.,

$$(\text{load})_{\text{slat}} \propto \underset{\downarrow\downarrow\downarrow}{\rho U_e^2\theta_e} - \underset{\downarrow\downarrow\downarrow}{\rho U_\infty^2\theta_\infty}$$

momentum loss due to load on slat upper surface

momentum loss due to zero load on slat upper surface

where Θ_∞ is the momentum thickness at the slat trailing edge in the absence of a pressure gradient on the slat upper surface, or after nondimensionalizing

$$\frac{\text{load on slat}}{\rho U_\infty^2\theta_\infty} \propto \frac{\rho U_e^2\theta_e - \rho U_\infty^2\theta_\infty}{\rho U_\infty^2\theta_\infty}$$

$$C_{L_{(SLAT)}} \propto \frac{\rho U_e^2\theta_e - \rho U_\infty^2\theta_\infty}{\rho U_\infty^2\theta_\infty} \tag{13}$$

In a similar manner it can be shown that the load on the main component is proportional to the sum of the following parameters, i.e.,

$$\text{load}_{\text{main component}} \propto \rho U_i^2\theta_{iu} + \rho U_i^2\theta_{iL}$$

or after nondimensionalizing

$$C_{L_{(\text{main component})}} \propto \frac{\rho U_i^2\theta_{iu} + \rho U_i^2\theta}{\rho U_\infty^2 C_{\text{slat}}} \tag{14}$$

Thus, from proportionality equations (13) and (14), $C_{L(MAX)}$ total is a function of the following two groups of non-dimensional parameters, i.e.,

$$C_{L_{(MAX)}} = F\left(\frac{\rho U_e^2\theta_e - \rho U_\infty^2\theta_\infty}{\rho U_\infty^2\theta_\infty}, \frac{\rho U_i^2\theta_{iu} + \rho U_i^2\theta_{iL}}{\rho U_\infty^2 C_{\text{slat}}}\right) \tag{15}$$

The equations shows the functional representations for $C_{L(MAX)}$ of a two-component system with a leading edge device. However, actual functional relations between these two parameters for $C_{L(MAX)}$ prediction must be established from experimental data. Figure 8 shows this relation as derived from experimental boundary-layer velocity profile data.

Some trends as shown by Fig. 8 are worth mentioning. If for a given slot exit velocity, the momentum loss in the slot flow at exit plane is higher, i.e., if the velocity profile of the slot efflux flow is fully developed, then a lower momentum loss in the outer boundary layer and a consequent lower slat load is required for achieving a desired value for $C_{L(MAX)}$. If the momentum loss of the slot stream exit is lower or negative (addition of energy as in the case of a blown system), then much higher slat loads as well as the load on the main component are allowed thus giving higher $C_{L(MAX)}$. This phenomena is also illustrated in Figure 8. However, this only holds as long as the slot exit velocity is greater than the velocity at the trailing edge of the upper component. If the slot exit velocity becomes less than the velocity on the upper component, $C_{L(MAX)}$ decreases because of the flow separation on the aft component.

IV. Results and Discussion

A. Single Component Airfoil

The onset of laminar stall on an airfoil section is highly dependent on three factors, namely 1) the level of leading edge peak pressure, 2) pressure gradient immediately downstream of the pressure peak near the leading edge, and 3) of equal importance, the value of the local momentum thickness Reynolds number $[U_{e(x)}\Theta_{(x)}]/\nu$ immediately downstream of the pressure peak. A typical airfoil which may exhibit a laminar stall at an angle of attack α_1, as an example, at freestream Reynolds number of 1 to 2 million, may either have laminar stall at a higher angle of attack $\alpha_2(\alpha_2 > \alpha_1)$ or may have trailing edge stall when the freestream Reynolds number is increased to, say, more than 6 million. In either case, whether a typical airfoil exhibits a laminar stall or a trailing edge stall, $C_{L(MAX)}$ is increased for the case of single component airfoil as the freestream Reynolds number is increased. However, in the case of a multicomponent airfoil this is not necessarily a valid statement because of the existence of a confluent boundary layer on the upper surfaces of various components of such an airfoil.

Figures 9a–11 show the results of a correlation study performed to determine the validity of the laminar stall criterion as programed on the digital computer. Three NACA airfoils were used to conduct the correlation, namely NACA 63-009, NACA 63-012, and NACA 64A010 of Ref. 15–19, respectively. In addition, the application of this criterion is demonstrated in modifying the sections of a three-dimensional wing for delaying the onset of laminar stall. For the purpose of correlation, the pressure distribution calculated by the potential flow program[14] was used in place of experimental pressure distribution. The reason for this was, that in many instances, the minimum peak pressure location on correlation airfoils did not coincide with the pressure pickups, resulting in loss of the actual pressure peak. For this reason, as well as the need for a refined definition of local pressure gradient (i.e., close point spacing), a potential flow computer program was used to generate the pressure distribution required for the study of these correlation airfoils. With the pressure data introduced into a laminar stall computer program, the existence of short bubble and bubble burst was determined through the use of criterion of Fig. 6. Local Mach number gradient, $[d\ M_e/d\ (S/C)]$, was calculated with a sliding curve fit applied to the values of M_e vs S/C. The slope of this curve was then found to give the gradient of local Mach number M_e with respect to the nondimensional distance on the surface of airfoil, S/C. Local momentum thickness Reynolds number $(U_e\ \Theta/\nu)$ was computed from the momentum thickness, Θ, supplied by the laminar boundary layer subroutine calculations. Both U_e and M_e are known from the local pressure coefficients.

Figures 9b, 10, and 11 show $C_L - \alpha$ curves, both theoretical and experimental for the NACA 63-009, 63-012, 64A010 and modified 64A010 airfoil sections. From the shape of these experimental $C_L - \alpha$ curves, it is evident that all of the above airfoil sections exhibit laminar stall. In all cases, it is observed from the computer program output, that the point of theoretical laminar separation on the airfoil surface occurs at an angle of attack several degrees lower than the stall angle of attack. This suggests the formation of short bubble and reattachment of separated shear layer. As the angle of attack is increased from the value of theoretical laminar separation occurrence, the criteria of Fig. 6 is used to predict the angle of attack at which bubble bursts and the flow completely separates from the surface of the airfoil, i.e., the occurrence of laminar stall.

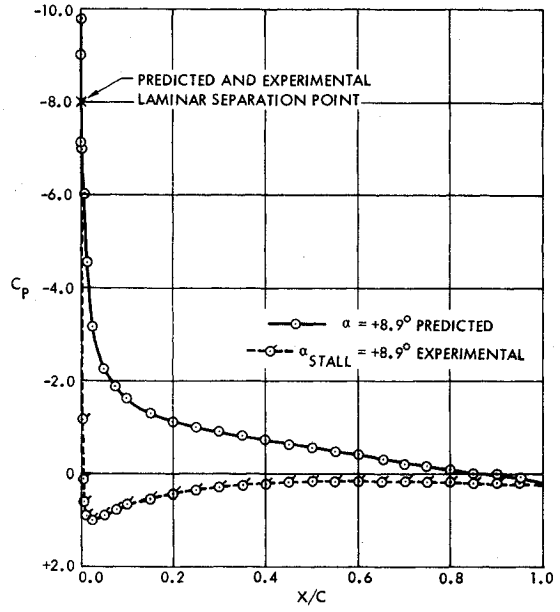

Fig. 9a Comparison of predicted and experimental leading edge stall. NACA 63-009 section $R_N = 58 \times 10^6$.[15]

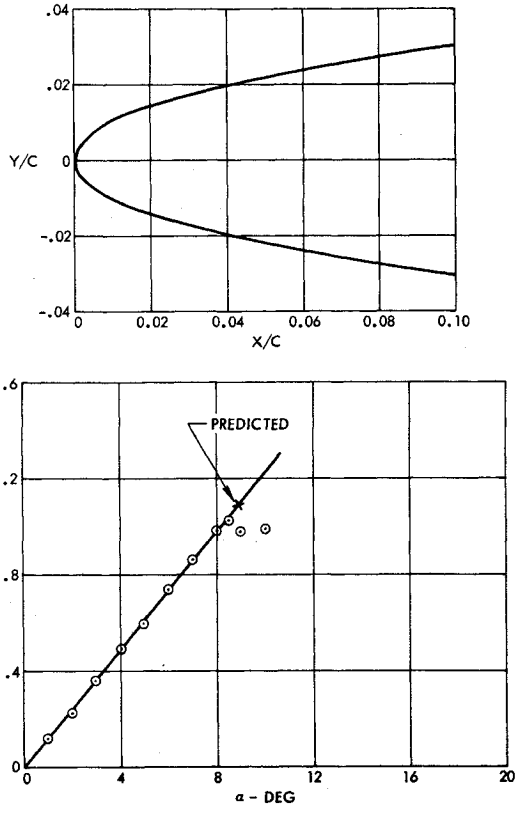

Fig. 9b Lift curves for NACA 63-009 section with predicted leading edge stall point.[15]

Figure 9a shows the comparison of the experimental and theoretical pressure distribution on NACA 63-009 airfoil section along with the experimental and predicted laminar separation point location. As is evident, the comparison between experimental and theory is quite good. Figure 9b shows the comparison of experimental and theoretical lift curve slopes and the angle of attack for laminar stall. Thus it is seen that the criterion of Fig. 6 leads to reasonable prediction of the angle of attack for laminar stall. Figure 10 shows the comparison of $C_L - \alpha$ curves for

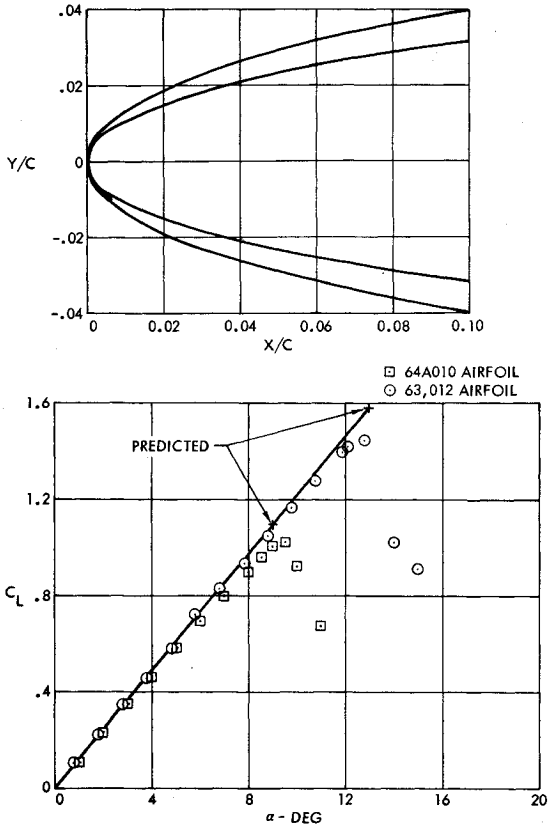

Fig. 10 Lift curves for NACA 63-012 and 64A010 sections with predicted leading edge stall points.[16,17]

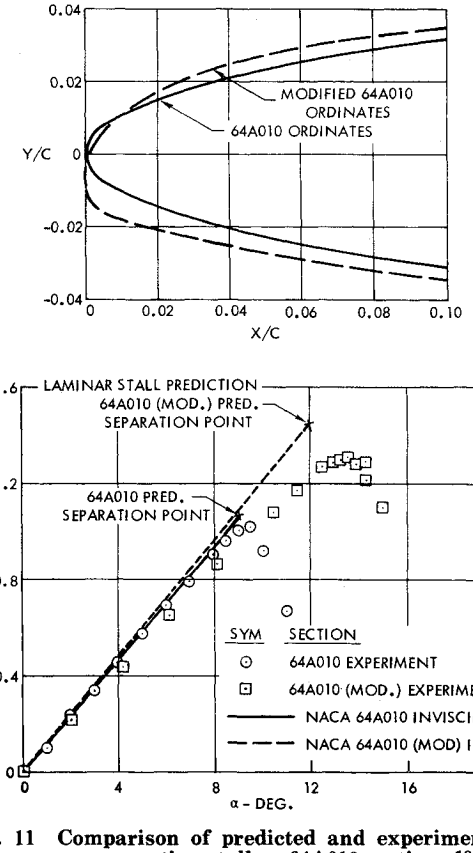

Fig. 11 Comparison of predicted and experimental laminar separation stall on 64A010 sections.[19]

NACA 63-012 and 64A010 airfoil sections. The two nose shapes drawn to scale illustrate that the thicker nose shape increases the value of $C_{L(MAX)}$. The effect of a mod-

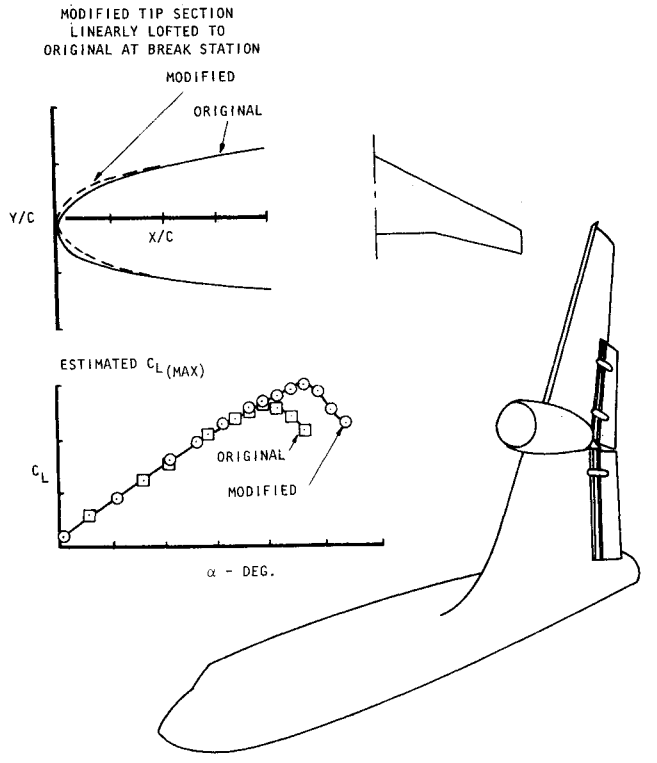

Fig. 12 Application of two-dimensional $C_{L(MAX)}$ criteria to the development of three-dimensional high lift system.

ification of the leading edge shape for the same thickness airfoil, i.e., for NACA 64A010, is clearly demonstrated in Fig. 11. The leading edge radius has been blunted and the nose thickened somewhat, resulting in higher value of $C_{L(MAX)}$ due to laminar stall. It is thus seen from Figs. 9b, 10, and 11 that the laminar stall criterion of Fig. 6 is successfully able to predict all these effects. This fact has been used to advantage in wing design for delaying the occurrence of laminar stall on a three-dimensional wing. Figure 12 illustrates the manner in which the leading edge shapes of wing sections were altered by the use of the criterion of Fig. 6 and simple sweep theory. As seen from this figure, wind-tunnel test results show the increment of 20% in $C_{L(MAX)}$ due to the above modifications.

B. Two-Component Airfoil with Leading Edge Slat

The curve for the relation between parameters for determining $C_{L(MAX)}$ of a two component airfoil section with leading edge slat is shown in Fig. 8. This curve was developed from the experimental data of Ref. 20. This curve was used in the frame work of multiple airfoil program[14] for predicting the $C_{L(MAX)}$ value for the NACA 64A010 airfoil section with leading edge slat.[21,22] Figure 13 shows the predicted values of the $C_L - \alpha$ curve by the multiple airfoil computer program with experimental data; in addition, a predicted value of $C_{L(MAX)}$ by the use of criterion of Fig. 8 is shown in this figure. The agreement, in this case, between the predicted and experimental value of $C_{L(MAX)}$ is satisfactory. Figure 14 shows the viscous pressure distribution computed by the computer program of Ref. 14 and an angle of attack near stall and comparison with experimental data. Comparison between the computed viscous pressure distribution and experimental data is excellent.

It is to be emphasized here that the criterion of Fig. 8 for the prediction of $C_{L(MAX)}$ for a two component airfoil with leading edge slat is suggested criterion which has been proven valid for the case shown in Fig. 13. However, in order to prove its full validity, more correlation work is needed.

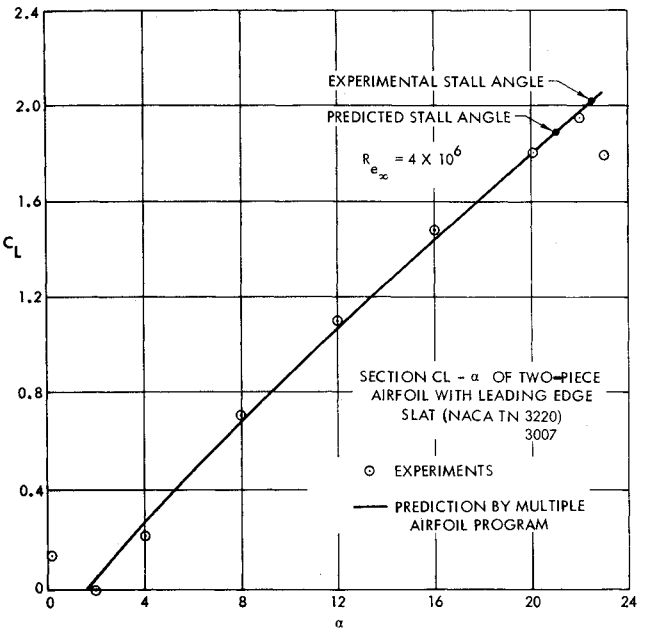

Fig. 13 Prediction of $C_{L(MAX)}$ for a two-component airfoil with a leading edge device by criterion of Fig. 8.

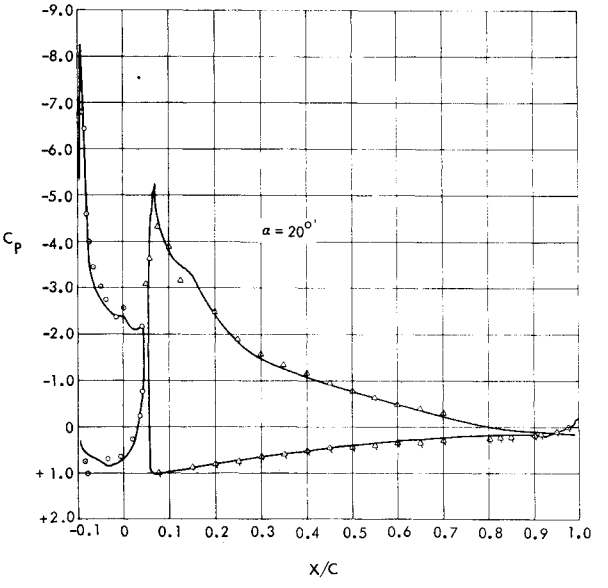

Fig. 14 Comparison of predicted pressure distribution on 64A010 airfoil having leading edge slat with experimental data.

Conclusions

1) From the theoretical analysis it has been shown that both pressure gradient and local Reynolds number based on momentum thickness at the point of theoretical laminar separation point are necessary to predict the reattachment of a laminar shear layer. The functional relationship, shown in Fig. 6, between the above parameters, derived from the velocity profile data in the vicinity of a laminar separation bubble, is able to predict laminar stall on the arbitrary airfoil section quite successfully.

2) For a two component airfoil with a leading edge slat, the single component airfoil criterion for $C_{L(MAX)}$ gives values of $C_{L(MAX)}$ that are too low. A criterion based on momentum losses in the boundary layer at the slat end has been suggested. This suggested criterion is successful in predicting $C_{L(MAX)}$ for the case of NACA 64A010 airfoil with leading edge slat. However, further work is needed in

this area for the purpose of designing a better leading edge system.

3) The effect of compressibility has been ignored in the theoretical analysis. However, this effect is pronounced and becomes important when dealing with the stall problem at high speeds, for example, in the case of transonic maneuvering.

References

[1]Jones, B. M., "An Experimental Study of the Stalling of Wings," ARC. R&M 1588, Dec. 1963, Aeronautical Research Council, London, England.

[2]Jones, B. M., "Stalling." *Journal Aerospace Society* Vol. 38, Sept. 1934, pp. 753–770.

[3]von Doenhoff, A. E., "A Preliminary Investigation of Boundary Layer Transition Along a Flat Plate with Adverse Pressure Gradient, TN 639, March 1938, NACA.

[4]McGregor, I., "Leading Edge Bubble on Sharp and Blunt Nosed Aerofoils," Ph.D. thesis, 1954, Queen Mary College, London.

[5]Owen, P. R. and Klanfer, L., "On the Laminar Boundary Layer Separation from the Leading Edge of a Thin Aerofoil," ARC. CP 220, 1955, Aeronautical Research Council, London, England.

[6]Crabtree, L. F., "The Formation of Regions of Separated Flow on Wing Surfaces, Part II, Laminar-Separation Bubbles and the Mechanisms of the Leading-Edge Stall," ARC. R&M 3122, 1959, Aeronautical Research Council, London, England.

[7]Crabtree, L. F., "The Formation of Regions of Separated Flow on Wing Surfaces; Part I, Low Speed Tests on a Two-Dimensional Upswept Wing with a 10-Percent Thick RAE 101 Section," RAE. Rept. Aero 2528 Nov. 1953, Royal Aircraft Establishment, Farnborough, England; reissued as Part I of ARC. R&M 3122, 1959, Aeronautical Research Council, London, England.

[8]Gaster, M., "The Structure and Behavior of Laminar Separation Bubbles," NPL. Aero Rept. 1181, Aug. 1966, National Physical Lab., England.

[9]Pohlhausen, K., "Zur näherungsweisen Integration der Differential-gleichung der laminaren Reibungsschicht," *Zeitschrift agnew. Mathematik und Mechanik.*, Vol. 1, 1921, pp. 252–268.

[10]Holstein, H. and Bohlen, T., "Ein einFaches verFahren zur Berechnung laminarer Reibungsschichten, die dem Näherungsansatz von K. Pohlhawen genügen," Lilienthal—Bericht S10, 1940, pp. 5–16.

[11]Schlichting, H. and Ulrich, A., "Zur Berechung des Umschlages laminar-turbulent," *Jahrbuch d. dt. LuftFahrt Forschung*, Vol. 1, No. 8, 1942.

[12]Granville, P. S., "The Calculation of Viscous Drag of Revolution," The David Taylor Model Basin Rept. 849, 1953, Navy Dept., Washington, D.C.

[13]Cohen, C. B. and Reshotko, E., "Similar Solutions for the Compressible Laminar Boundary Layer with Heat Transfer and Pressure Gradient," Rept. 1293, 1956, NACA.

[14]Stevens, W. A., Goradia, S. H., and Braden, J. A., "Mathematical Model for Two-Dimensional Multi-Component Airfoils in Viscous Flow," CR-1843, July 1971, NASA.

[15]Gault, D. E., "Boundary-Layer and Stalling Characteristics of the NACA 63-009 Airfoil Section, TN-1894, NACA.

[16]McCullough, G. B. and Gault, D. E., "An Experimental Investigation of an NACA 63-012 Airfoil Section with Leading Edge Suction Slots, TN-1683, 1948, NACA.

[17]Peterson, R. F., "The Boundary-Layer and Stalling Characteristics of the NACA 64A010 Airfoil Section," TN 2235, Nov. 1950, NACA.

[18]Altman, J. M. and Hayter, N. L. F., "A Comparison of the Turbulent Boundary-Layer Growth on an Unswept and a Swept Wing," TN-2500, Sept. 1951, NACA.

[19]Maki, R. L. and Hunton, L. W., "An Investigation at Subsonic Speeds of Several Modifications to the Leading Edge Region of the NACA 64A010. Airfoil Section Designed to Increase Maximum Lift," TN-3871, Dec. 1956, NACA.

[20]Goradia, S. H., "Confluent Boundary Layer Flow Development with Arbitrary Pressure Distribution," Ph.D. thesis, Aug. 1971, Mechanical Engineering Dept., Georgia Inst. of Technology, Atlanta, Ga.

[21]Kelly, J. and McCullough, G., "Aerodynamic Loads on a Leading Edge Flap and a Leading Edge Slat on the NACA 64A010 Airfoil Section," TN-3220, June 1954, NACA.

[22]Kelly, J. and Hayter, N. L., "Lift and Pitching Moment at Low Speeds of the NACA 64A010 Airfoil Section Equipped with Various Combinations of L.E. Slot, L.E. Flap, Split Flap, and Double Slotted Flap," TN-3007, Sept. 1953, NACA.

[23]Goradia, S. H. and Bennett, J. A. "Method of Analysis for Airfoils at Subsonic Mach Numbers with Some Transonic Applications," developed under contract with Army Research Organization, Rept. ARO-D-348, July 1966, Arnold Air Force Station, Tenn.

[24]Baker, J. V., "Boundary Layer Transition on the NACA 0012 and 23012 Airfoils in the 8-Foot High Speed Wind Tunnel, WR-L-682, 1940, NACA.